Effect of surface roughness and temperature on stainless steel - whey protein interfacial interactions under pasteurisation conditions

Avila-Sierra, Alejandro; Zhang, Jason; Fryer, Peter

DOI:
10.1016/j.jfoodeng.2021.110542
10.1016/j.jfoodeng.2021.110542

Journal of Food Engineering

Title

Effect of surface roughness and temperature on stainless steel - whey protein interfacial interactions under pasteurisation conditions

Authors

Alejandro Ávila-Sierra, Zhenyu Jason Zhang, and Peter J. Fryer*

Address

School of Chemical Engineering, University of Birmingham, Edgbaston, Birmingham B15 2TT, United Kingdom

Corresponding authors

Peter J. Fryer ***E-mail address:*** p.j.fryer@bham.ac.uk

Keywords

Milk fouling, surface free energy, temperature, roughness, adhesion, polarity.

Acknowledgements

The research team acknowledges the School of Chemical Engineering, University of Birmingham, for financial support and provision of a studentship. We are also grateful for funding from the CSEF project that is funded by EPSRC (EP/K011820/1). ZJZ thanks EPSRC for financial support (EP/P007864/1).

Abstract

The effects of the surface characteristics of 316L stainless steel (SS316L), including chemical composition before and after foulant deposition, surface roughness, and wall temperature, on both the liquid-solid and the solid-solid interfacial interactions have been investigated using contact angle measurements and atomic force microscopy respectively. Wettability of the metal surface was favoured by increased surface roughness (in the range-limited for food contact applications) and wall temperature (within the temperature range used for pasteurisation). A fine surface finish (i.e. mirror) could be an effective intervention to reduce liquid adhesion and the subsequent foulant deposition, especially under thermal treatment. The surface free energy (SFE) of SS316L and its polar and disperse components remained constant from ambient to pasteurisation temperatures (< 80°C). However, as fouling develops, the surface free energy evolved: upon foulant deposition, SFE decreased. An increased polarity (3.4% from 25 to 80°C) of the fouled surface could be related to the exposure the hydrophobic core of reversibly adsorbed β-Lactoglobulin toward the foulant-air interface. Both surface adhesion and Young's modulus at sub-micron spatial resolution confirmed that the packing within the foulant and molecular orientation on the foulant surface were affected by the temperature of the underlying substrate. Temperature also affected the wetting behaviour of cleaning solutions on surface foulant; as the surface temperature increased from 25°C to 75°C, the contact angle on WPC increased, suggesting an enhanced surface hydrophobicity. Overall, this work highlights the importance of surface parameters on governing the interfacial interactions that are competing for the control of the complex fouling phenomena.

Highlights

- Surface free energy and polarity of stainless steel remains constant over the range of operational temperatures (25 ~ 80°C).
- Surface free energy decreases upon foulant deposition.
- Polarity of the model proteinaceous foulant increases as temperature increases.
- Foulant hydrophobicity increases as the wall temperature increases.
- Liquid-surface temperature difference affects the mechanical characteristics of the deposit formed.

Graphical Abstract

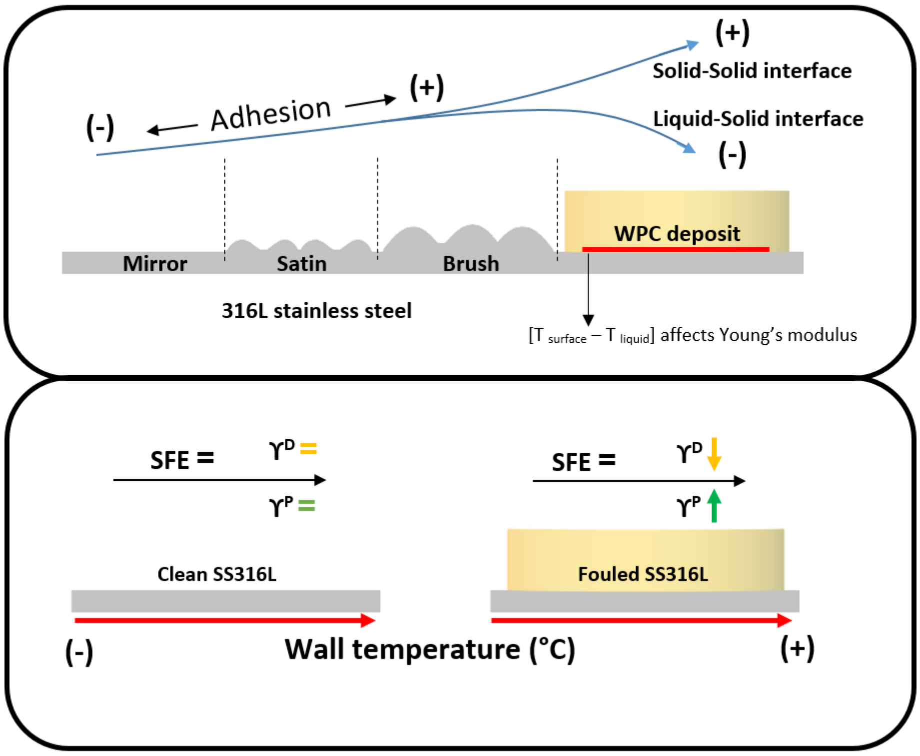

1. Introduction

In the dairy industry, surface fouling within pasteurisation equipment results in serious challenges for maintaining the performance of processing lines. Extensive cleaning operations are often required, which has a significant impact on the total production cost (Van Asselt et al., 2005). The cost to address issues related to heat-exchanger fouling for industrialised countries was estimated as 0.25% of the country gross national product (GNP) (Garrett-Price et al., 1985). This financial cost, alongside other issues such as product contamination, environmental impact, and industrial sustainability, emphasises the urgent need to understand fouling.

Food manufacture commonly involves equipment made of stainless steel, amongst which austenitic 304 and 316L are mostly used due to their chemical neutrality and physical durability (Schmidt et al., 2012). A range of studies have been carried out to understand and fabricate hierarchically structured surfaces, with much less attention paid to realistic engineering surfaces (Kubiak et al., 2011). The surfaces involved in a manufacturing process, including the welded joints, would be polished to meet the hygienic criteria of the installation, but even though surface roughness is well defined for food applications ($Ra \leq 0.80$ µm) (Frantsen and Mathiesen, 2009), subtle variations could considerably affect interfacial interactions, especially under processing conditions.

Fouling results from interactions between the products being processed and the surfaces in contact with them, whose characteristics govern deposition and the magnitude of interfacial adhesion. At the macroscopic scale, interfacial adhesion is commonly related to surface wettability, the ability of a liquid to wet a solid surface, and contact angle measurements are used to predict the amount of foulant deposited (Handojo et al., 2009; Williams et al., 2005). The wettability of a solid substrate is determined by the balance between cohesive forces (Work of cohesion: W_c) and adhesive forces of the liquid on a solid surface (Work of adhesion: W_a) (Choi et al., 2002): if $W_a > W_c$, the liquid spreads over the surface, and vice versa. However, surface wettability can be altered by surface characteristics such as topography (Avila-Sierra et al., 2019; Zhang et al., 2015) and temperature gradients (Karapetsas et al., 2017).-Kubiak et al. (2011) investigated a broad spectrum of surfaces, including metallic, ceramic and polymeric ones, reporting that there was a minimum contact angle below Ra < 1 μm associated with the droplet spreading along the polishing grooves.

Contact angle measurements can be also used to quantify surface free energy (SFE), viewed as a critical fouling precursor. The SFE of a given substrate offers a direct measure of the intermolecular interactions at the interface (Zhao et al., 2004), and strongly influences the adsorption/adhesion behaviour of compounds (such as proteins (Boxler et al., 2013; Rosmaninho and Melo, 2008), cells and bacteria (Baier, 1980; Tsibouklis et al., 2000), starches (Białopiotrowicz, 2003) and minerals (Boxler et al., 2013; Rosmaninho and Melo, 2008, 2006a)). A correlation was established between the electron-donor component of the substrate and the final amount of deposit formed (Rosmaninho and Melo, 2006b), where surfaces with low energy less favourable for binding (Rosmaninho and Melo, 2006b; Tsibouklis et al., 2000; Zhao et al., 2007). The weaker binding at the interface, the easier the cleaning process (Akesso et al., 2009). Baier et al. (1985) demonstrated the importance of both temperature and SFE on bacterial adhesion at 37°C. However, very few SFE studies have studied common engineering surfaces, particularly at working temperatures. Zhao et al. (2004) measured the surface free energy of 304 stainless steel, alongside some other amorphous carbon surfaces, from 20 to 95°C, and reported that there were significant SFE variations when the testing temperature was above 80°C. In addition to determining the effects that surface free energy and temperature might have on surface fouling, it is critical to understand the influence that other physical (e.g.

polishing process) and chemical transformations (e.g. foulant deposition) on the metal surface might have on the interfacial interactions involved amid food processing.

During milk thermal treatment, β-Lactoglobulin (β-Lg) unfolds and exposes its hydrophobic core containing reactive disulphide and sulfhydryl bonds (Claeys et al., 2001) that can react rapidly with the processing equipment and other bulk fluid compounds (Bansal and Chen, 2006). At the nanoscale, atomic force microscopy (AFM) can determine the force/work of adhesion between a wide variety of surfaces (e.g. stainless steel, ceramic, mineral, glass and poly(tetrafluoroethylene)) (Akhtar, 2010; Navabpour et al., 2010; Sauerer et al., 2016; Verran et al., 2000) and has been used to study food confectionary foulants such as Turkish delight, caramel and sweetened condensed milk (Akhtar et al., 2010). These works highlighted differences between adhesion forces as a function of surface type, while others showed that adhesion of substrates can be measured by AFM at real process temperatures (Capella and Stark, 2006; Goode et al., 2013). When temperature increases, the work of adhesion tends to increase, especially for proteinaceous deposits that are denatured upon heating (Goode et al., 2013).

The influence of surface parameters (i.e. roughness, SFE, and temperature) on surface fouling is clear, but identifying their synergetic effects, especially under realistic conditions, will provide further insights to reduce industrial fouling. This work studies the effects of surface characteristics of 316L stainless steel on surface fouling, from nano- to macro-scale, by characterisation of surface properties before and after foulant deposition under simulated pasteurisation conditions. The objectives are (i) to determine the influence of surface characteristics on adhesion between liquid and solid (SS or foulant), (ii) to determine the extent of surface hydrophobicity as a function of surface fouling, and (iii) to establish connections between the mechanical properties of both substrates, stainless steel and foulant, and the surface parameters examined.

2. Materials & methods

2.1 Surface characterisation

Stainless steel 316L surfaces (2.54 x 2.54 cm) were prepared by using different sandpapers grit (600, 240, and 180 for mirror, satin and brush grades respectively). The process produces unidirectionally oriented substrates within the standard roughness limit defined by the 3-A Sanitary Standards (3-A SSI) and the European Hygienic Engineering & Design Group (EHEDG) for dairy industries (Ra < 0.8 μm) (Frantsen and Mathiesen, 2009). Surface roughness (Ra) was determined by White Light Interferometry (WLI) (MicroXAM2, Omniscan, U.K.) from at least four locations on each sample.

Stainless steel coupons were cleaned by the method detailed in Phinney et al., (2017): 2.0% (wt./wt.) NaOH aqueous solution at 80°C under stirring for 1 h to achieve complete removal of potential contaminants, and cooled to room temperature using a water bath. The substrates were subsequently rinsed by 1.0% (vol./vol.) HCl solution, soaked in hexane for 5 min and then acetone for another 5 min before dried by an air stream. All solvents used are HPLC grade.

2.2 Fouling material and procedure

A commercial whey protein concentrate (WPC) (CARBELAC 35, Carbery, Cork, Ireland) was used as received to prepare a model foulant solution (10% wt./wt.) to which the polished stainless steel coupons were exposed. Specifications of the WPC powder used are listed in **Table 1.** The model solution was prepared by mixing the WPC powder with de-ionised water at room temperature for an hour. Attention was paid to minimise aeration, foam formation, and proteins denaturation of the solution following the procedure developed in Phinney et al., (2017). To mimic relevant industrial conditions (pasteurisation temperatures, protein denaturation and surface contact time allowing ageing of the deposit), 1 ml of the prepared solution was placed on the cleaned coupons (temperature kept at 25°C before deposition, unless otherwise stated) and maintained at 75°C for 1 h in an oven, and then cooled. Time and temperature profiles were used to minimise bubble formation, allowing gelation of the solution (Phinney et al., 2017). Average fouling thickness and roughness were measured by WLI from at least four different areas, and surface topography characterised using an AFM (Dimension 3100, Veeco, Cambridge, UK) in Tapping mode using silicon cantilevers (HQ:NSC15/AlBS AFM tip; ApexProbes, UK).

Table 1. Chemical composition and protein profile of the commercial WPC powder. For chemical specification, percentage is expressed by grams of component per 100 g of WPC powder. For protein profile, percentage is expressed by grams of proteins per 100 g of True Protein. Data supplied by Carbery (Ballineen, Co Cork, Ireland).

Chemical Specification	**Total concentration (%)**
Protein	35.0
Total Nitrogen	5.5
Moisture	5.0
Fat	4.0
Ash	6.0
Lactose	50.0
Protein profile	
Glycomacropeptide / Caseinomacropeptide	27.1
α -lactalbumin	7.5
Blood Serum Albumin	4.5
β-lactoglobulin	56.7
Lactoferrin	2.0
Immunoglobulin G	2.1

2.3 Contact angle measurements and surface free energy characterisation

The sessile drop method was deployed to measure the equilibrium contact angle (ECA) for wall temperatures between 25 to 80°C. ECA was quantitatively measured on a stage where the influence of convective motion is negligible. A small liquid droplet was placed on the solid substrate while contact angle evolution was recorded in real-time (1000 fps) by a high-speed camera (FastCam SA2, Photron Europe, Bucks, United Kingdom). Stainless steel coupons (with or without foulant) were placed on a heating stage monitored by a digital thermometer and controlled by a thermal bath. A pipette was used to place 10 μL droplets of the testing liquids on the substrate when the surface temperature is constant. ImageJ software was used for image processing.

The set of test liquids in **Table 2** has been selected to emphasize specific molecular interactions of the surfaces of interest: two non-polar liquids (diiodomethane and 1-bromonaphthalene) were selected to characterise non-polar interactions, while a polar liquid (Ethylene glycol) is used to model the solid surface as having two components to its surface energy, polar and non-polar.

The **Wu method** (Wu, 1973, 1971) was selected for calculating the surface free energy (SFE) of a solid substrate by dividing it into polar and disperse components. This Harmonic mean model provides reliable values of both disperse and polar parts. The liquids used were 1-Bromonaphthalene and ethylene glycol. The equations used for calculations are:

$$\gamma_{\mathrm{sl}} = \gamma_{\mathrm{s}} + \gamma_{\mathrm{l}} - \frac{4\gamma_{\mathrm{s}}^{\mathrm{d}}\gamma_{\mathrm{l}}^{\mathrm{d}}}{\gamma_{\mathrm{s}}^{\mathrm{d}}+\gamma_{\mathrm{l}}^{\mathrm{d}}} - \frac{4\gamma_{\mathrm{s}}^{\mathrm{p}}\gamma_{\mathrm{l}}^{\mathrm{p}}}{\gamma_{\mathrm{s}}^{\mathrm{p}}+\gamma_{\mathrm{l}}^{\mathrm{p}}} \qquad [1]$$

Combining [1] with Young's equation, the following equation can be obtained:

$$\gamma_{\mathrm{l}}(1 + \cos\mathrm{ECA}) = \frac{4\gamma_{\mathrm{s}}^{\mathrm{d}}\gamma_{\mathrm{l}}^{\mathrm{d}}}{\gamma_{\mathrm{s}}^{\mathrm{d}}+\gamma_{\mathrm{l}}^{\mathrm{d}}} - \frac{4\gamma_{\mathrm{s}}^{\mathrm{p}}\gamma_{\mathrm{l}}^{\mathrm{p}}}{\gamma_{\mathrm{s}}^{\mathrm{p}}+\gamma_{\mathrm{l}}^{\mathrm{p}}} \qquad [2]$$

Where ECA is the equilibrium contact angle, Υ_{sl} is the interfacial tension between the solid and the liquid, Υ_{s} is the overall surface energy of the solid, and Υ_{l} is the overall surface tension of the wetting liquid, along with their corresponding disperse (Υ^{D}) and polar components (Υ^{P}).

Table 2. Properties of liquids used to characterise the equilibrium contact angle. Properties listed as a function of temperature: total surface tension of the liquid (γ_L^T), and corresponding disperse (γ_L^D) and polar components (γ_L^P).

Liquid	T (°C)	Formula	γ_L^T (mN/m)	γ_L^D (mN/m)	γ_L^P (mN/m)
Diiodomethane (Landolt and Börnstein, 1961)	25	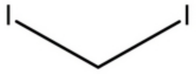	50.0	50.0	0.0
	80		42.5	42.5	0.0
1-Bromonaphthalene (Rulison, 2005)	25	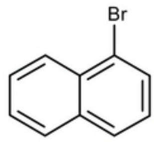	44.6	44.6	0.0
	80		42.2	42.2	0.0
Ethylene glycol (MEGlobal, 2008)	25	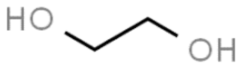	47.5	28.7	18.8
	80		43.6	26.3	17.3

2.4 Nano-mechanical characterisation of substrates

Nano-mechanical properties of all surfaces were quantified by atomic force microscope (AFM) (Dimension 3100, Veeco, Cambridge, UK) based force spectroscopy. A borosilicate microsphere, with a nominal diameter of 5.9 µm (Thermo Fisher Scientific, Loughborough, UK), was fixed to an AFM cantilever (ApexProbes, UK) using an epoxy adhesive (Araldite, UK) that is chemically inert. Spring constant of each cantilever was quantified using the thermal method (Hutter and Bechhoefer, 1993). Force measurements were carried out over four different locations per sample, with at least 50 force curves at each location. Adhesion force was quantified by the hysteresis upon retraction of the particle from the surface in contact. Indentation Analysis (NanoScope Analysis), using the Hertz model (spherical indenter) and fitting by the Contact Point Based method, was used to calculate Young's modulus of the substrates of interest. This method emphasises the minimum force at the contact point while minimising the influence of noise and interferences. Poisson's ratio was assumed to be 0.477 for Whey protein gels (Langley and Green, 1989) and 0.270 for SS316L surface (AZoNetwork UK Ltd, Manchester, United Kingdom).

2.5 Liquid cohesion and adhesion work

The work of cohesion (W_c) is defined as the work per unit area produced in dividing a pure liquid (**Eq. 3**), while the work of adhesion (W_a) is defined (**Eq. 4**) as the work required to separate two adjacent phases, in this case, a liquid-solid system (Ebnesajjad, 2006). If the ratio Wc/Wa is below one, the liquid spreads along the surface because adhesion work is larger than the cohesive one.

$$W_{\mathrm{c}} = 2\gamma_{\mathrm{L}} \quad [3]$$

$$W_{\mathrm{a}} = \gamma_{\mathrm{L}}(1 + \cos\mathrm{ECA}) \quad [4]$$

2.6 Statistical analysis: ANOVA

One-way analysis of variance (ANOVA) (Gelman, 2005) of both liquid contact angle and SFE of stainless steel surfaces was carried out as a function of both surface roughness and temperature to identify statistical differences between the means of two or more groups.

3. Results & Discussion

3.1 Effect of surface temperature and roughness on stainless steel wettability

Stainless steel (316L) coupons were processed to achieve three different surface finishes based on their roughness level (R_a): mirror (0.03 ± 0.01 µm); satin (0.31 ± 0.01 µm); and brush (0.83 ± 0.13 µm), for which the wettability was measured as a function of both wall temperature and liquid type. Droplets of three different liquids, ethylene glycol (EG), bromonaphthalene (BN), and diiodomethane (DM), were placed on the stainless steel coupons for contact angle measurements. ECA values are summarised in **Figure 1**. It was assumed that liquid droplets completely wet the metal surface according to Wenzel (1936) (no air entrapped).

Temperature directly influences liquid properties such as surface tension, density and viscosity (Escobedo and Mansoori, 1996; Wandschneider et al., 2008). At room temperature, contact angles decreased according to liquid surface tension; DM showed the highest contact angle (43.0 ± 1.8°; **Figure 1b**). At higher temperatures (25-80°C), ECAs decreased. The contact angles of EG and BN were most reduced as surface temperature increased. One-way ANOVA analysis was performed (**Table 3**), and shows significant ECA differences for EG and BN as a function of temperature. However, the wetting properties of DM did not seem to change with temperature despite its surface tension being more sensitive to the temperature than the other liquids (**Table 2**).

Surface roughness ($Ra < 0.83$ µm) appeared to affect the ECA measurements under the testing conditions: the rougher the surface, the greater the wetting observed. ANOVA analysis shows insignificant differences for ECA values of both EG and BN as a function of substrate roughness. However, the ECA results of DM was very responsive to roughness variations. These differences may be related to the spreading factor of those liquids (Kubiak et al., 2011).

Surface parameters play an important role in interfacial adhesion. Wetting of SS316L increases as a function of both the surface roughness and temperature. Industrially, these results imply that polishing surfaces to a high finish is effective in reducing liquid adhesion, and subsequent fouling: this agrees with practice, as well as previous experimental works where significant fouling reduction was observed using a mirror-finish surface instead of an unpolished one (Zouaghi et al., 2018).

Figure 1. Equilibrium contact angle (ECA) as a function of both SS316L roughness and temperature. Three classes of surface finish have been used: mirror, satin, and brush. The mean values of liquid contact angles of at least three different drops per liquid are showed along standard deviation. The liquid used are 1-bromonaphthalene (a), diiodomethane (b) and ethylene glycol (c). Lines show linear regression fit to facilitate data visualisation.

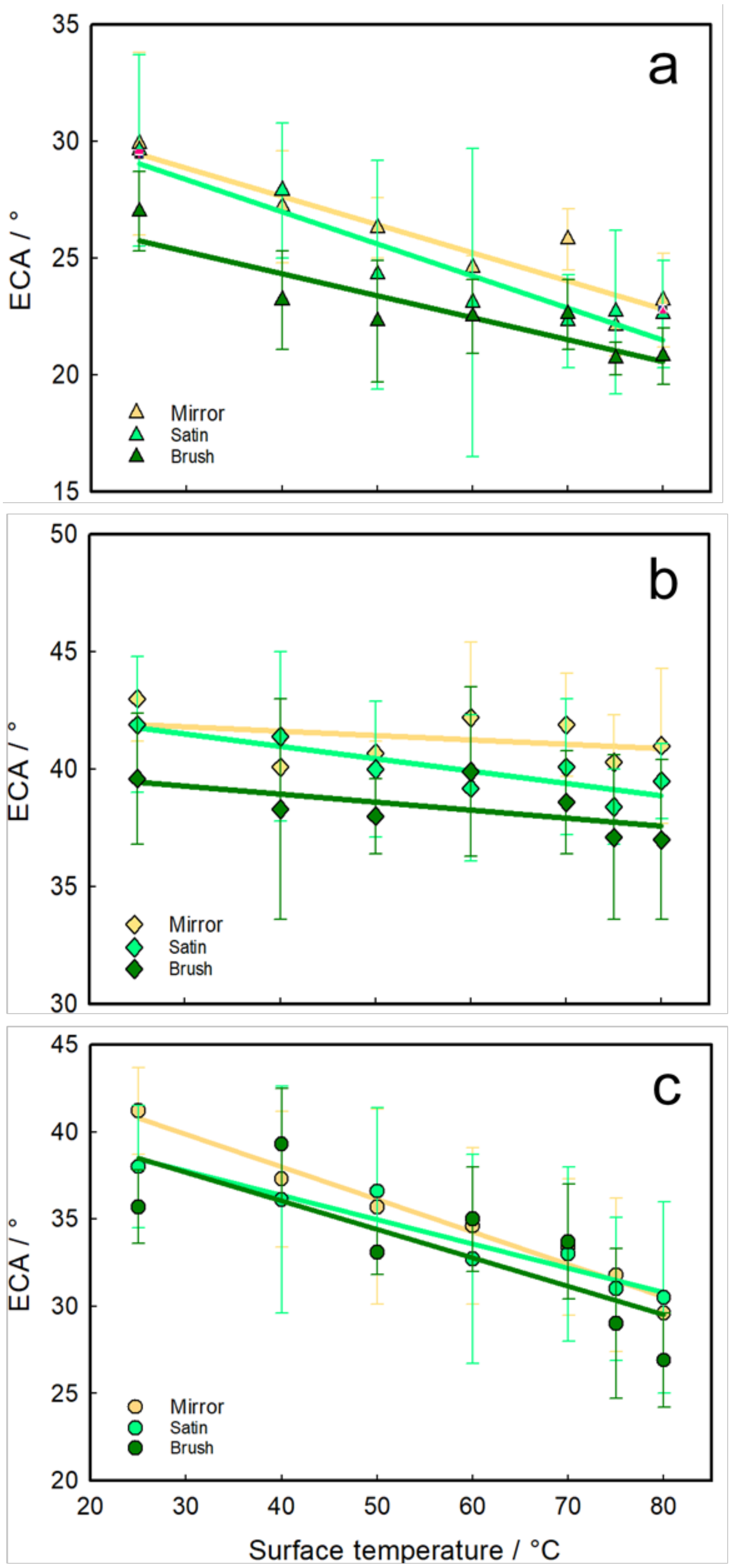

Table 3. One-way ANOVA analysis of both Equilibrium Contact Angle (ECA) and Surface Free Energy (SFE) measurements of clean and fouled 316L stainless steel as a function of surface temperature and roughness. F-value and p-value refer to the ratio of the variance of the group means to pooled within group variance and the probability of obtaining an F-value, respectively. P-value must be <0.05 to show a statistical significant difference between groups for the studied conditions.

	Temperature dependence		**Roughness dependence**	
	F-Value	*p-Value*	*F-Value*	*p- Value*
ECA upon SS316L				
Diiodomethane	1.0996	0.4098	6.9074	0.0059
1-Bromonaphthalene	5.7781	0.0033	2.4257	0.1167
Ethylene glycol	8.1499	0.0006	0.6341	0.5418
SFE of SS 316L				
Total	0.4156	0.8566	10.1399	0.0011
Disperse	0.5533	0.7599	12.5021	0.0004
Polar	1.4503	0.2645	0.3753	0.6924
ECA upon foulant				
Diiodomethane	0.4958	0.6952		
1-Bromonaphthalene	0.0349	0.9906		
Ethylene glycol	4.8457	0.0330		
SFE of WPC foulant				
Total	0.0915	0.9627		
Disperse	0.4989	0.6933		
Polar	6.3722	0.0163		

3.2 Alteration of surface wettability upon deposition of WPC foulant

3.2.1 Roughness of the surface foulant

Whey protein foulant was prepared on the polished stainless steel coupons, simulating a well-formed proteinaceous layer of similar characteristics to pasteuriser deposits. The areal density and averaged thickness of this model foulant were 17.67 mg/cm^2 (Phinney et al., 2017) and 105.8 ± 8.6 µm respectively, which is consistent with the values for averaged fouling of raw milk after eight hours of pasteurisation (12.73 ± 0.65 mg/cm^2 ; SS316L plate of Ra 0.46 ± 0.2 µm) found by Barish and Goddard (2013). Surface morphology of the whey protein foulant, acquired by AFM in ambient conditions, are presented in **Figure 2**. The mean foulant roughness measured by WLI is 23 ± 6 nm, 23 ± 10 nm and 22 ± 8 nm on SS substrates with mirror, satin, and brush finishes respectively, close to that measured by AFM (12.4 ± 0.8 nm over a 20 × 20 µm area). A high resolution 3D scan (**Figure 2b)** shows that the clusters are of sizes less than 0.3 µm, agreeing with the previous work (Jimenez et al., 2013). The consistent surface roughness values of foulants suggests that the influence of the surface finish of the underlying substrate is negligible for the model foulants formed. This is likely because the thickness of the foulant far exceeds the magnitude of the roughness of the coupons used. As such, the effect of WPC foulant roughness was neglected for contact angle measurements.

Figure 2. Representative surface morphology images of WPC foulant prepared at 75°C for 1 hour on stainless steel coupons of (a) mirror (20 × 20 µm); (b) mirror (3D image 1 × 1 µm); (c) satin and (c) brush finishes.

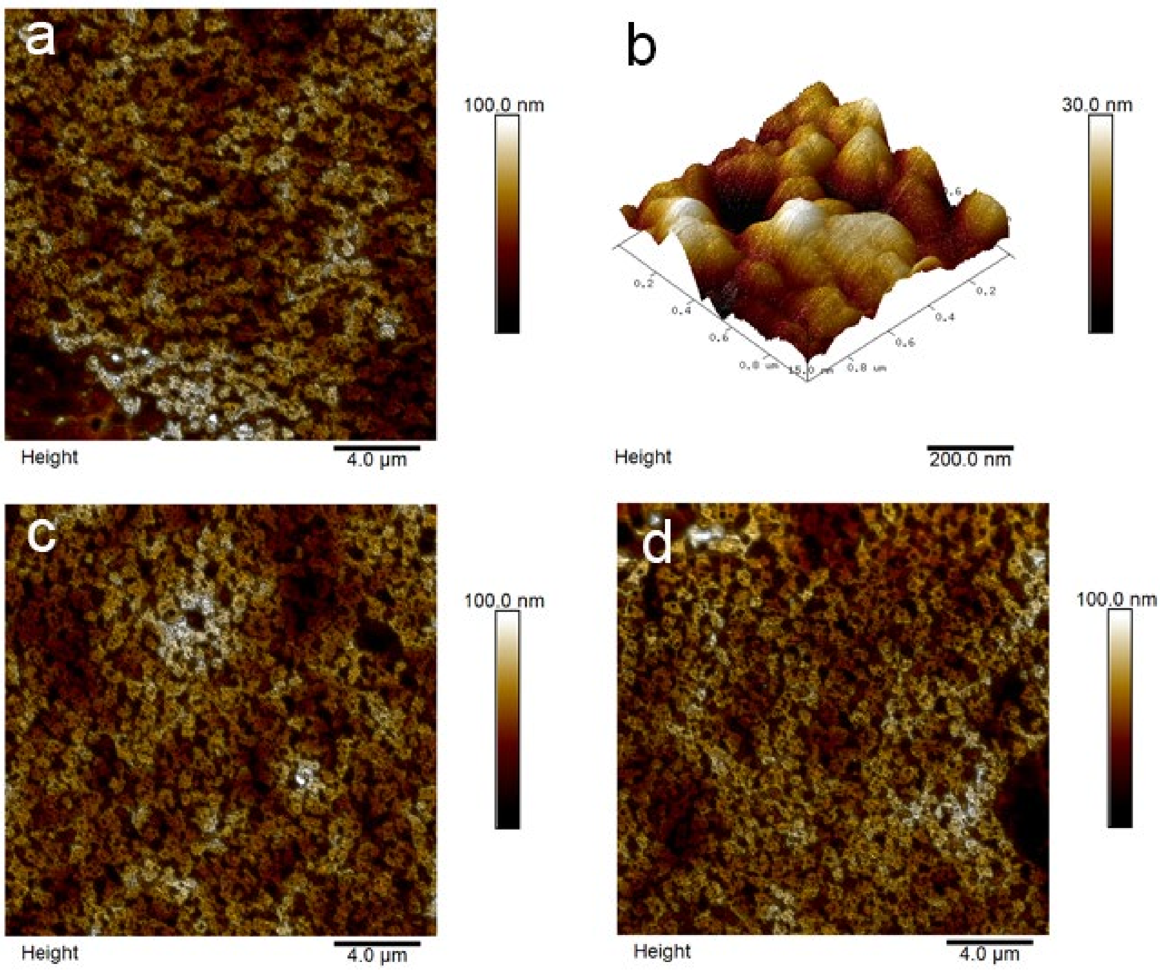

3.2.2 Contact angle measurements of pure liquid as a function of foulant temperature

Denaturation and aggregation reactions of β-Lactoglobulin (β-Lg) that occur at pasteurisation temperatures lead to reactions of β-Lg with processing equipment and with other bulk compounds. β-Lg adsorption and its adhesion force are favoured by increased surface temperature (Santos et al., 2003). This section aims to examine the wetting characteristics of the model foulant layer as a function of wall temperature and liquid type.

Figure 3 presents the wettability of both stainless steel and foulant as a function of temperature for the three testing liquids, which shows temperature dependence for both substrates. The ECA of non-polar liquids remained constant as the temperature increases: DM showed greater contact angle than BN (41.90 ± 3.24° and 37.72 ± 2.69° respectively) throughout the temperature range examined. While the ECA of DM was constant for both substrates, that of BN on the foulant was almost 10 degrees greater than on the bare metal surface. Although the contact angle of BN on the stainless steel coupons decreased by ca. 6° when the temperature was increased from 25 to 80°C, it remained nearly constant (± 0.38°) on the WPC deposit over the same temperature range.

The polar liquid, EG, showed the highest value at room temperature (60.0 ± 2.0°), suggesting a significant reduction of surface energy at the foulant-liquid interface. When the temperature of the substrate increased, the magnitude of reduction in the ECA of EG was similar for both metal and foulant. However, the ECA of EG on stainless steel was ca. 20 degrees greater than on the formed foulant. Of the three liquids tested, EG is the only one that shows such significant statistical differences with increased temperature (**Table 3**), which suggests that changes of polar and disperse interactions could be important once foulant is formed. A proteinaceous foulant layer can alter the wettability of a substrate as a function of both liquid composition and wall temperature.

Surface wettability is determined by the balance between adhesive and cohesive interactions at the solid-liquid interface. The ratio between the works of cohesion and adhesion of the liquids tested over the mirror-finish stainless steel substrates is presented in **Table 4**.

For non-polar liquids, there is a reduction of the disperse forces inside the liquid drop as temperature increases, promoting liquid spreading across the metal substrate. The constant contact angles of the non-polar liquids on the foulant is likely due to reduction of the disperse interactions, that compensate the temperature influence. For the polar liquid, increasing temperature reduces the polar and disperse bonds inside the liquid, reducing cohesive interactions and favouring surface wetting. It is clear that temperature has a much greater influence on the ECA on the foulant than on the SS substrate, related to the increased polarity at the interface.

Once total spreading of liquid was observed on the prepared foulant, drops of the two non-polar liquids were stable at short contact times (minutes), and there was no significant dissolution on the protein layer. However, the solubility of the polar liquid was favoured considerably over contact time. This supports the hypothesis that polarity might be critical for understanding the foulant-liquid interface.

Figure 3. Equilibrium contact angle (ECA) of the three selected liquids, 1-Bromonaphthalene, Diiodomethane, and Ethylene glycol as a function of temperature. Comparison of ECA evolution upon both substrates, (a) stainless steel and (b) WPC foulant. Error bars represent the standard error from at least three measurements.

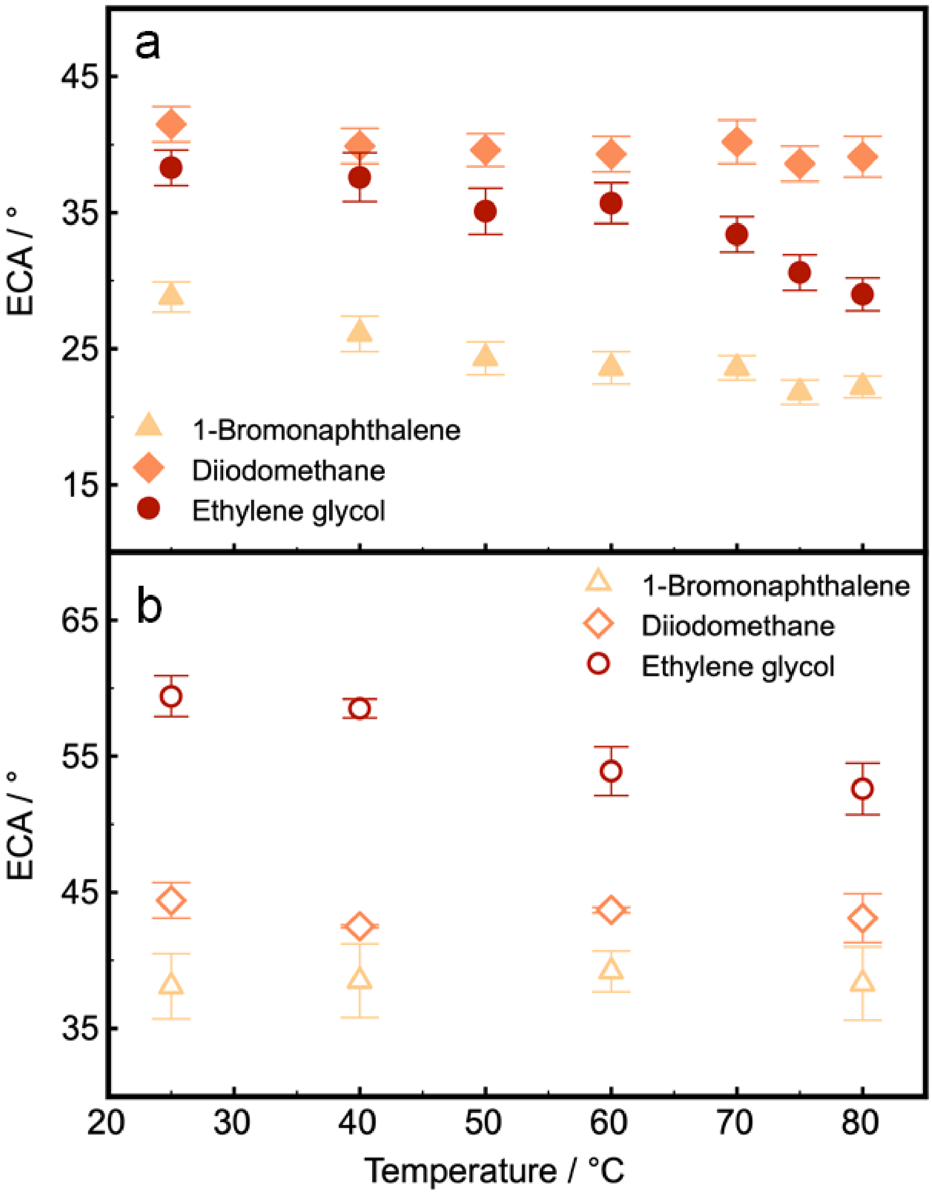

Table 4. Ratio of cohesion and adhesion work (**section 2.5**) for liquids as a function of temperature on the substrates of interest (stainless steel and WPC fouling). Large ratio ($W_{cohesion}/W_{adhesion} > 1$) suggests that the liquid has less tendency to spread on the substrate under the given condition, and vice versa.

			[W_c/ W_a]	
	T [°C]	***DM***	***BN***	***EG***
SS316L (mirror)				
	25	1.16	1.07	1.14
	40	1.13	1.06	1.13
	50	1.12	1.06	1.12
	60	1.10	1.05	1.11
	70	1.08	1.05	1.10
	75	1.07	1.04	1.10
	80	1.07	1.04	1.09
	Reduction	*0.09*	*0.03*	*0.05*
WPC foulant				
	25	1.15	1.12	1.33
	40	1.15	1.12	1.31
	60	1.15	1.12	1.27
	80	1.14	1.12	1.23
	Reduction	*0.01*	*0.00*	*0.10*

3.2.3 Contact angles of cleaning solution on WPC foulant

As shown in **Figures 1** and **3**, it is likely that temperature will have a significant influence on the wetting behaviour of the cleaning solutions on the surface foulant, which determines the removal mechanisms. **Figure 4** shows the contact angles of different cleaning formulations, including water and aqueous solutions of different NaOH concentration (0.5%, 1% and 2% wt./wt.), on the WPC foulant as a function of the surface temperature (25, 50 and 75°C).

At room temperature (25°C), water contact angle on the WPC foulant was found to be 49.0 ± 5.2°, slightly less than on a clean stainless steel surface (66.8 ± 9.0° for mirror and 52.4 ± 5.4° for brush finishes). This is very likely due to solvation of the proteinaceous film upon contact with water. As the temperature increased from 25°C to 75°C, the contact angle of water on WPC increased, suggesting an enhanced surface hydrophobicity, a different characteristic to that observed on bare stainless steel (**Figure 3**) where high temperature facilitated surface wetting of water. Because the prepared WPC foulant consists of densely packed proteins, we speculate that the adsorbed β-Lactoglobulin either exposed its hydrophobic core to the foulant-air interface or denaturated at increased temperature, giving increased surface hydrophobicity of the WPC. Contact angles of cleaning solutions followed a similar behaviour, and according to the ANOVA test in **Table 5**, there was no significant difference between ECAs of water and the cleaning solutions tested. This observation highlights the critical role of molecular configuration on the foulant surface in determining its wettability. Previous work suggested that fast foulant removal was observed at a high temperatures (Phinney et al., 2017), which confirms that cleaning is a complex process determined by not only the surface wettability of the foulant, but its cohesiveness and its adhesion to the supporting substrate (stainless steel here).

Figure 4. Contact angle measurements of cleaning liquids upon WPC foulant as a function of wall temperature (25, 50, and 75°C). The cleaning solutions are water, NaOH 0.5%, NaOH 1%, and NaOH 2%. ANOVA analysis shows non-significant differences between CAs of the cleaning solutions tested.

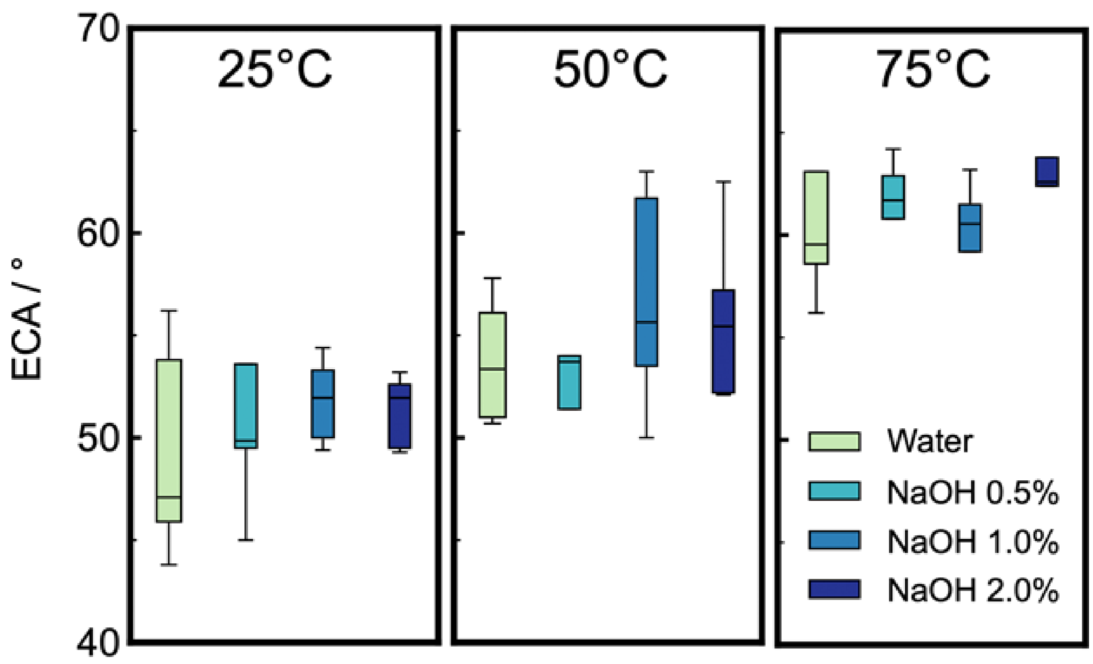

Table 5. One-way ANOVA analysis of the effect of both cleaning formulations and substrate temperature on the wettability of WPC fouled stainless steel 316L. F-value and p-value refer to the ratio of the variance of the group means to pooled within group variance and the probability of obtaining an F-value, respectively. P-value must be <0.05 to show a statistical significant difference between groups for the studied conditions.

	Temperature dependence	
	F-Value	*p-Value*
Water	3.6823	0.0006
NaOH 0.5%	3.6823	0.0005
NaOH 1%	3.6823	0.0010
NaOH 2%	3.6823	0.0000
	Effect of cleaning formulation	
	F-Value	*p-Value*
25°C	3.0984	0.5085
50°C	3.0984	0.4525
75°C	3.0984	0.5069

3.3 Surface free energy of stainless steel and WPC foulant

Figure 5 shows that the total surface free energy of the SS316L substrate, as well as its disperse and polar components, are independent of surface temperature (45.4 ± 0.6, 39.4 ± 0.5, and 6.0 ± 0.4 mN/m respectively). The measured values of SFE are in agreement with those reported at room temperature (Barish and Goddard, 2013; Zhao et al., 2004). ANOVA analysis (**Table 3**) suggests that the polar component has no notable dependence on surface roughness and temperature, whilst the disperse component is affected by surface roughness. A previous study concerning the effects of both roughness and temperature on SFE (Avila-Sierra et al., 2019) showed that the greater surface roughness, the higher the surface energy.

Our results confirm that the SFE of stainless steel surfaces is constant in the operational window of industrial pasteurisation processes, which implies that the attractive interactions between stainless steel and the liquid being processed remain constant. SFE at room temperature could be used to estimate the free energy of the substrate under 80°C. However, other parameters such as surface roughness or alterations of liquid properties do affect the interfacial interactions.

The pasteurisation process, however, is more dynamic than the contact angle measurements carried out in the present study – SFE of the solid substrate would evolve as the foulant develops. It is therefore critical to evaluate the SFE of a model proteinaceous layer as the function of temperature, upon which the underpinning formation mechanism of the foulant can be established. The effect of temperature on the liquid-foulant interface is of particular interest. Harmonic mean approach (**section 2.3**) was implemented to evaluate the SFE variations up to 80°C, with data of **Figure 5** confirming that the total SFE of the foulant remained constant (38.0 ± 0.1 mN/m), consistent with the observation made on stainless steel. However, the dispersive and polar components of the SFE changed: there is a slight decrease of the dispersive part while the polar part increases significantly, showing an increase of the foulant polarity around 3.4% from 25 to 80°C (calculated as % of $\gamma_{S_{Polar}}/\gamma_{S_{Total}}$). ANOVA analysis (**Table 3**) shows significant differences for the polar part once temperature increased. These findings support our hypothesis that the adsorbed β-Lactoglobulin could adjust its molecular configuration so as to expose the hydrophobic core, leading to an increased surface polarity.

Some previous studies confirmed the relationship between an increased amount of foulant and the polar component of a wide variety of surfaces (e.g. diamond-like carbon (DLC) coatings (Boxler et al., 2013), imbedded MoS_2^{2+} ions, SiOx and DLC–Si–O films, Ni–P matrix with PTFE particles (Rosmaninho and Melo, 2008), TiN layers (Rosmaninho et al., 2005), and implantation of SiF_3^+ ions (Rosmaninho et al., 2007; Rosmaninho and Melo, 2006b)), where a secondary protein layer could develop on the initially bound protein film through polar interactions (Addesso and Lund, 1997). However, temperature not only affects fouling rate and polarity of the deposit, it also affects deposit itself (Burton, 1968). As a result of increased wall temperature, the increased polarity of the surface foulant might accelerate the interactions between compounds at the bulk fluid and the pre-deposited material, which explains why minerals tend to present in the first layer of protein deposit (Belmar-Beiny and Fryer, 1993), forming a compacted structure over the processing time (Pappas and Rothwell, 1991).

During milk processing, the rate of heat transfer decreases with time due to the build-up of surface foulant (Kukulka and Leising, 2009). Alharthi (Alharthi, 2014) identified how the concentration of proteins and minerals can affect such reduction. Therefore, after the development of the surface deposit, heat transfer will decrease due to the deposit thickness/composition, generating a gradient of temperature inside the deposit. This implies alterations of temperature that would limit the molecular interactions at the interface, and hence minimise the fouling rate over time.

Figure 5. (a) Disperse, (b) Polar, and (c) Total Surface Free Energy of both SS316L (filled) and WPC foulant (empty) as a function of wall temperature. Liquids tested: Ethylene glycol and 1-Bromonaphthalene. Error bars represent the standard error of at least three measurements.

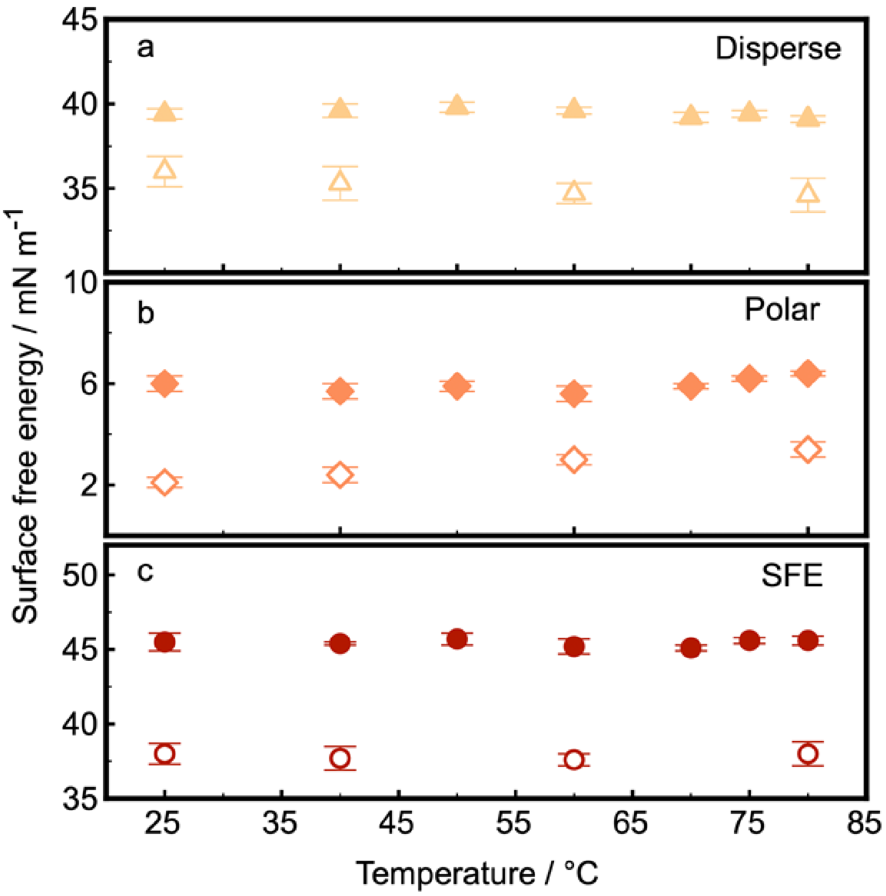

3.4 Effect of the roughness and deposition temperature on the nanomechanical properties of the substrate

Results suggest that the liquid-solid interface is controlled by surface parameters such as roughness and wall temperature, whilst the surface free energy data confirms that the temperature of the solid substrate influences the characteristics of the formed foulant in terms of polarity and hydrophobicity. To further decouple the effects of chemistry and roughness on the surface free energy, force spectroscopy experiments based on AFM were carried out in ambient on SS316L substrates of different finishing grades, data presented in **Figure 6a**. As demonstrated (Sauerer et al., 2016), such a technique can be effectively used as an alternative to conventional contact angle experiments with significantly improved spatial resolution. The adhesion measured between a colloidal probe (diameter ca. 6 µm) and substrate in an ambient environment is primarily determined by the capillary force that is controlled by the humidity of the environment, chemical composition, roughness, and modulus of the substrate.

For stainless steel samples, both environmental conditions and chemical composition were kept constant, and the contact area is approximately 0.056 μm^2, assuming Hertzian contact mechanics. Adhesion force on the SS substrates with mirror finish was in the range 1.5-2.5 µN, consistent with that on SS of satin finishing, but with a slightly broader distribution, as shown in **Figure 6a**. The similar range of adhesion measured on the mirror and satin samples suggests that the effect of roughness on surface energy at sub-micron scale was insignificant between those two finishes. The averaged surface adhesion increased to 3.5 µN, with a broad distribution, on the SS substrate with brush finish. Enhanced surface adhesion was likely due to the elevated contact area between the colloidal probe and the solid surface, as the result of increased surface roughness, evidenced by both the surface morphology and the scattered distribution of the adhesion force.

Figure 6. Adhesion force between an AFM colloidal probe and both (a) 316L stainless steel with mirror, satin, and brush surface finishes and (b) the WPC foulant generated on 316L SS with mirror finish under controlled surface temperature: 25°C, 50°C and 75°C.

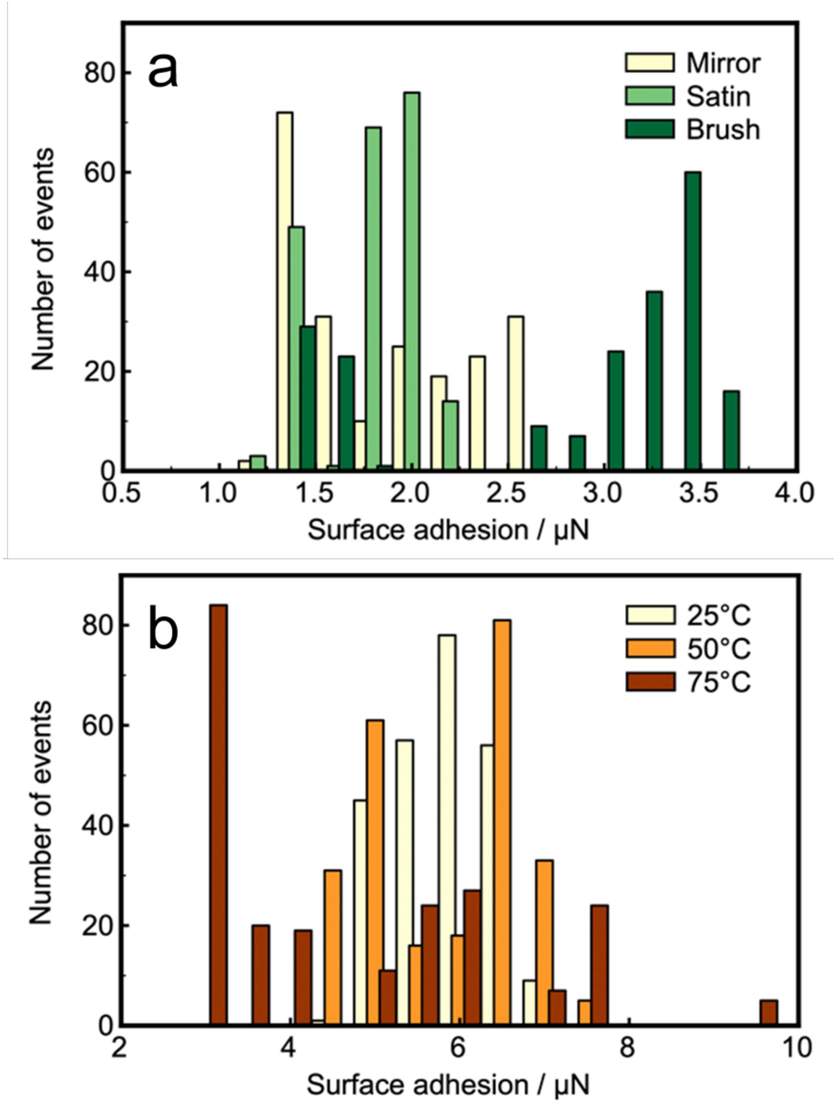

Figure 6b shows the histograms of adhesion force acquired from the proteinaceous foulant developed on SS substrates of mirror finish at three different substrate temperatures. In the presence of the WPC foulant, it is clear that the surface adhesion was increased to a range of 3-10 μN: of the several parameters that determine the surface adhesion, foulant roughness probably plays only a small role, as evidenced by the morphology in **Figure 2**. The polar groups on the surface of the foulant, are likely the major contributing factor for increased adhesion,

consistent with the contact angle results presented in **Figure 3**. Although there was only minor difference between average adhesion measured on foulants formed at 25 and 50°C, there was an increased range of adhesion force on the latter. This increased further on foulant prepared at 75°C: adhesion force spanned a broad range, implying a heterogeneous surface, likely the result of increasingly random molecular orientation.

The cohesiveness of the formed foulant and its correlation with the surface parameters and the processing conditions, can be quantified by using AFM based nanoindentation. The Young's modulus (YM) of the foulant was quantified as a function of temperature. The synergistic effect of surface roughness and deformability (Young's modulus) determines the contact area between two surfaces (Halvey et al., 2018; Rabinovich et al., 2000). At room temperature, there is a reduction in YM from 3.9 ± 0.7 GPa to 3.3 ± 1.3 GPa for clean and fouled mirror SS substrates respectively, where both materials can be viewed as hard substrates (Halvey et al., 2018). For proteinaceous foulants deposited on the SS with the three different metal finishes, the averaged YM remains practically constant (3.3 ± 1.3 GPa and 3.2 ± 0.4 GPa for both fouled mirror and brush metal surfaces respectively), independent of the roughness of the supporting substrate. However, Young's modulus of the WPC foulant increased with temperature: 3.3 ± 1.3 GPa, 3.7 ± 0.3 GPa and 3.9 ± 0.7 GPa for 25, 50 and 75°C respectively, likely due to the configuration of protein molecules during deposition. This again highlights the impact the first foulant layer could have on the overall deposit characteristics. It is probable that the WPC proteins would form a densely packed foulant layer, with less uniform molecular orientation, when exposed to a mirror polish SS substrate at high temperature (75°C), whilst they would construct a less densely packed and more homogeneous surface film at 25°C.

4. Conclusions

This work demonstrates that surface roughness, temperature, changes in surface composition, as well as the temperature difference between liquid and substrate govern the interfacial interactions in fouling, and therefore will control initial and subsequent formation of surface layers. Wettability of 316L stainless steel is favoured by increased surface roughness and wall temperature, showing how fine surface finishes are effective in reducing fouling. The surface free energy (SFE) of SS316L and its components remain constant between ambient and pasteurisation temperatures. However, as fouling develops, the SFE evolves. Upon foulant deposition, SFE decreases, and there was a polarity increase (3.4% from 25 to 80°C) of the fouled surface that might relate to the opening of the hydrophobic core of β-Lactoglobulin toward the foulant-air interface. Both surface adhesion and Young's modulus at sub-micron spatial resolution confirm that the molecular packing within the foulant and the molecular orientation on the foulant surface are affected by the temperature of the underlying substrate, showing how temperature variations in an industrial heat exchanger can result in different surface deposits.

References

Addesso, A., Lund, D.B., 1997. Influence of soild surface energy on protein adsorption. J. Food Process. Preserv. 21, 319–333. https://doi.org/10.1111/j.1745-4549.1997.tb00786.x

Akesso, L., Pettitt, M.E., Callow, J.A., Callow, M.E., Stallard, J., Teer, D., Liu, C., Wang, S., Zhao, Q., D'Souza, F., Willemsen, P.R., Donelly, G.T., Kocijan, A., Jenko, M., Jones, L.A., Guinaldo, P.C., 2009. The potential of nano-structured silicon oxide type coatings deposited by PACVD for control of aquatic biofouling. Biofouling 25, 55–67. https://doi.org/10.1080/08927010802444275

Akhtar, N., Bowen, J., Asteriadou, K., Robbins, P.T., Zhang, Z., Fryer, P.J., 2010. Matching the nano- to the meso-scale: Measuring deposit–surface interactions with atomic force microscopy and micromanipulation. Food Bioprod. Process. 88, 341–348. https://doi.org/10.1016/j.fbp.2010.08.006

Akhtar, N.R., 2010. The fundamental interactions between deposits and surfaces at nanoscale using atomic force microscopy. PhD thesis, University of Birmingham.

Alharthi, M., 2014. Fouling and cleaning studies of protein fouling at pasteurisation temperatures. PhD thesis, University of Birmingham.

Avila-Sierra, A., Zhang, Z.J., Fryer, P.J., 2019. Effect of surface characteristics on cleaning performance for CIP system in food processing. Energy Procedia 161, 115–122. https://doi.org/10.1016/j.egypro.2019.02.067

Baier, R.E., 1980. Substrata influences on the adhesion of microorganisms and their resultant new surface properties. G. Bitton, K.S. Marshall (Eds.), Adsorption of Microorganisms to Surfaces, Wiley-Interscience Publishers, New York, 59–104.

Baier, R.E., Depalma, V.A., Goupil, D.W., Cohen, E., 1985. Human platelet spreading on substrata of known surface chemistry. J. Biomed. Mater. Res. 19, 1157–1167. https://doi.org/10.1002/jbm.820190922

Bansal, B., Chen, X.D., 2006. A Critical Review of Milk Fouling in Heat Exchangers. Comprehensive reviews in food science and food safety. 5, 27–33. https://doi.org/10.1111/j.1541-4337.2006.tb00080.x

Barish, J.A., Goddard, J.M., 2013. Anti-fouling surface modified stainless steel for food processing. Food Bioprod. Process. 91, 352–361. https://doi.org/10.1016/j.fbp.2013.01.003

Belmar-Beiny, M.T., Fryer, P.J., 1993. Preliminary stages of fouling from whey protein solutions. J. Dairy Res.

6, 467–483. https://doi.org/10.1017/S0022029900027837

Białopiotrowicz, T., 2003. Wettability of starch gel films. Food Hydrocoll. 17, 141–147. https://doi.org/10.1016/S0268-005X(02)00046-2

Boxler, C., W., A., Scholl, S., 2013. Fouling of milk components on DLC coated surfaces at pasteurization and UHT temperatures. Food Bioprod. Process. 91, 336–347. https://doi.org/10.1016/j.fbp.2012.11.012

Burton, H., 1968. Reviews of the progress of dairy science. J. Dairy Res. 35, 317–330. https://doi.org/10.1017/S0022029900019038

Capella, B., Stark, W., 2006. Adhesion of amorphous polymers as a function of temperature probed with AFM force–distance curves. J. Colloid Interface Sci. 296, 507–514. https://doi.org/10.1016/j.jcis.2005.09.043

Choi, W.Y., Park, H.J., Ahn, D.J., Lee, J., Lee, C.Y., 2002. Wettability of chitosan coating solution on “Fuji” apple skin. J. Food Sci. 67, 2668–2672. https://doi.org/10.1111/j.1365-2621.2002.tb08796.x

Claeys, W.L., Ludikhuyze, L.R., Van Loey, A.M., Hendrickx, M.E., 2001. Inactivation kinetics of alkaline phosphatase and lactoperoxidase, and denaturation kinetics of β-lactoglobulin in raw milk under isothermal and dynamic temperature conditions. J. Dairy Res. 68, 95–107. https://doi.org/10.1017/S002202990000460X

Ebnesajjad, S., 2006. 2 - Surface Tension and Its Measurement. Surf. Treat. Mater. Adhes. Bond. 9–28. https://doi.org/10.1016/B978-081551523-4.50004-3

Escobedo, J., Mansoori, G.A., 1996. Surface Tension Prediction for Pure Fluids. AIChE J. 42, 1425–1433. https://doi.org/10.1002/aic.690420523

Frantsen, E., Mathiesen, J.T., 2009. Specifying Stainless Steel Surfaces for the Brewery, Dairy and Pharmaceutical Sectors, in: NACE Corrosion. p. 9573.

Garrett-Price, B., Smith, B., Watts, R., Knudsen, J., Marner, W., Suitor, J., 1985. Fouling of Heat Exchangers, Characteristics, Costs, Prevention, Control and Removal. Noyes Publ. Park Ridge, NJ.

Gelman, A., 2005. Analysis of variance—why it is more important than ever. Ann. Stat. 33, 1–53. https://doi.org/10.1214/009053604000001048

Goode, K.R., Bowen, J., Akhtar, N., Robbins, P.T., Fryer, P.J., 2013. The effect of temperature on adhesion forces between surfaces and model foods containing whey protein and sugar. J. Food Eng. 118, 371–379. https://doi.org/10.1016/j.jfoodeng.2013.03.016

Halvey, A.K., Macdonald, B., Dhyani, A., Tuteja, A., 2018. Design of surfaces for controlling hard and soft fouling. Philos. Trans. A 377, 2138. https://doi.org/10.1098/rsta.2018.0266.

Handojo, A., Zhai, Y., Frankel, G., Pascall, M.A., 2009. Measurement of adhesion strengths between various milk products on glass surfaces using contact angle measurement and atomic force microscopy. J. Food Eng. 92, 305–311. https://doi.org/10.1016/j.jfoodeng.2008.11.018

Hutter, J.L., Bechhoefer, J., 1993. Calibration of Atomic Force Microscope Tips. Rev. Sci. Instrum. 64, 1868. https://doi.org/10.1063/1.1143970

Jimenez, M., Delaplace, G., Nuns, N., Bellayer, S., Deresmes, D., Ronse, G., Alogaili, G., Collinet-Fressancourt, M., Traisnel, M., 2013. Toward the understanding of the interfacial dairy fouling deposition and growth mechanisms at a stainless steel surface: A multiscale approach. J. Colloid Interface Sci. 404, 192–200. https://doi.org/10.1016/j.jcis.2013.04.021

Karapetsas, G., Chamakos, N.T., Athanasios, O., Papathanasiou, G., 2017. Thermocapillary Droplet Actuation: Effect of Solid Structure and Wettability. Langmuir 33, 10838–10850. https://doi.org/10.1021/acs.langmuir.7b02762

Kubiak, K.J., Wilson, M.C.T., Mathia, T.G., Carra, S., 2011. Dynamics of contact line motion during the wetting of rough surfaces and correlation with topographical surface parameters. Scanning 33, 370–377. https://doi.org/10.1002/sca.20289

Kukulka, D.J., Leising, P., 2009. Evaluation of Surface Coatings on Heat Exchangers. Chem. Eng. Trans. 18, 339–344.

Landolt, H., Börnstein, R., 1961. Numerical Data and Functional Relationships in Science and Technology. New Ser. 16, 144.

Langley, K.R., Green, M.L., 1989. Compression strength and fracture properties of model particulate food composites in relation to their microstructure and particle-matrix interaction. J. Texture Stud. 20, 191–207. https://doi.org/10.1017/S0022029900026480

MEGlobal, 2008. Ethylene Glycol Product Guide.

Navabpour, P., Teer, D., Su, X., Liu, C., Wang, S., Zhao, Q., Donik, C., Kocijan, A., Jenko, M., 2010. Optimisation of the properties of siloxane coatings as anti-biofouling coatings: Comparison of PACVD and hybrid PACVD–PVD coatings. Surf. Coatings Technol. 204, 3188–3195. https://doi.org/10.1016/j.surfcoat.2010.03.011

Pappas, C.P., Rothwell, J., 1991. The effects of heating, alone or in the presence of calcium or lactose, on calcium binding to milk proteins. Food Chem. 42, 183–201. https://doi.org/10.1016/0308-8146(91)90033-K

Phinney, D.M., Goode, K.R., Fryer, P.J., Heldman, D., Bakalis, S., 2017. Identification of residual nano-scale foulant material on stainless steel using atomic force microscopy after clean in place. J. Food Eng. 214, 236–244. https://doi.org/10.1016/j.jfoodeng.2017.06.019

Rabinovich, Y., Adler, J.J., Ata, A., Singh, R.K., Moudgil, B.M., 2000. Adhesion between Nanoscale Rough Surfaces. J. Colloid Interface Sci. 232, 10–16. https://doi.org/10.1006/jcis.2000.7167

Rosmaninho, R., Melo, L.F., 2008. Protein–calcium phosphate interactions in fouling of modified stainless-steel surfaces by simulated milk. Int. Dairy J. 18, 72–80. https://doi.org/10.1016/j.idairyj.2007.06.008

Rosmaninho, R., Melo, L.F., 2006a. The effect of citrate on calcium phosphate deposition from simulated milk ultrafiltrate (SMUF) solution. J. Food Eng. 73, 379–387. https://doi.org/10.1016/j.jfoodeng.2005.02.017

Rosmaninho, R., Melo, L.F., 2006b. Calcium phosphate deposition from simulated milk ultrafiltrate on different stainless steel-based surfaces. Int. Dairy J. 16, 81–87. https://doi.org/10.1016/j.idairyj.2005.01.006

Rosmaninho, R., Rizzo, G., Muller-Steinhagen, H., Melo, L.F., 2005. Anti-fouling stainless steel based surfaces for milk heating processes, in: Proceedings of 6th International Conference on Heat Exchanger Fouling and Cleaning - Challenges and Opportunities.

Rosmaninho, R., Santos, O., Nylander, T., Paulsson, M., Beuf, M., Benezech, T., Yiantsios, S., Andritsos, N., Karabelas, A., Rizzo, G., Müller-Steinhagen, H., Melo, L.F., 2007. Modified stainless steel surfaces targeted to reduce fouling – Evaluation of fouling by milk components. J. Food Eng. 80, 1176–1187. https://doi.org/10.1016/j.jfoodeng.2006.09.008

Rulison, C., 2005. Effect of Temperature on the Surface Energy of Solids. KRUSS Application Note AN250e.

Santos, O., Nylander, T., Rizzo, G., Müller-Steinhagen, H., Trägårdh, C., Paulsson, M., 2003. Study of whey protein adsorption under turbulent flow rate, in: Proceedings of Heat Exchanger Fouling and Cleaning—

fundamentals and Applications. p. 24.

Sauerer, B., Stukan, M., Abdallah, W., Derkani, M.H., Fedorov, M., Buiting, J., Zhang, Z.J., 2016. Quantifying mineral surface energy by scanning force microscopy. J. Colloid Interface Sci. 472, 237–246. https://doi.org/10.1016/j.jcis.2016.03.049

Schmidt, R.H., Erickson, D.J., Sims, S., Wolff, P., 2012. Characteristics of Food Contact Surface Materials: Stainless Steel. Food Prot. Trends 32, 574–584.

Tsibouklis, J., Stone, M., Thorpe, A.A., Graham, P., Nevell, T.G., Ewen, R.J., 2000. Inhibiting bacterial adhesion onto surfaces: the non-stick coating approach. Int. J. Adhes. Adhes. 20, 91–96. https://doi.org/10.1016/S0143-7496(99)00034-2

Van Asselt, A.J., Vissers, M.M.M., Smit, F., De Jong, P., 2005. In-line control of fouling., Heat Exchanger Fouling and Cleaning—Challenges and Opportunities, Engineering Conferences International Kloster Irsee, Germany, 5-10 June (Engineering Conferences International, New York, USA).

Verran, J., Rowe, D.L., Cole, D., Boyd, R.D., 2000. The use of the atomic force microscope to visualise and measure wear of food contact surfaces. Int. Biodeterior. Biodegradation 42, 99–105. https://doi.org/10.1016/S0964-8305(00)00070-6

Wandschneider, A., Lehmann, J.K., Heintz, A., 2008. Surface Tension and Density of Pure Ionic Liquids and Some Binary Mixtures with 1-Propanol and 1-Butanol. J. Chem. Eng. Data 53, 596–599. https://doi.org/10.1021/je700621d

Wenzel, R.N., 1936. Resistence of solid surfaces to wetting by water. Ind. Eng. Chem. Res. 28, 988.

Williams, A.M., Jones, J.R., Paterson, A.H.J., Pearce, D.L., 2005. Milks and milk concentrates: surface tension measurement. Int. J. Food Eng. 1, 1556–3758. https://doi.org/10.2202/1556-3758.1002

Wu, S., 1973. Polar and Nonpolar Interactions in Adhesion. J. Adhes. 5, 39–55. https://doi.org/10.1080/00218467308078437

Wu, S., 1971. Calculation of interfacial tension in polymer systems: Polymer Symposia. J. Polym. Sci. Polym. Symp. 34, 19–30. https://doi.org/10.1002/polc.5070340105

Zhang, P., Wang, S., Wang, S., Jiang, L., 2015. Superwetting Surfaces under Different Media: Effects of Surface Topography on Wettability. Small nano micro 11, 1939–1946. https://doi.org/10.1002/smll.201401869

Zhao, G., Raines, A.L., Wieland, M., Schwartza, Z., Boyan, B.D., 2007. Requirement for both micron- and submicron scale structure for synergistic responses of osteoblasts to substrate surface energy and topography. Biomaterials 28, 2821–2829. https://doi.org/10.1016/j.biomaterials.2007.02.024

Zhao, Q., Liu, Y., Abel, E.W., 2004. Effect of temperature on the surface free energy of amorphous carbon films. J. Colloid Interface Sci. 280, 174–183. https://doi.org/10.1016/j.jcis.2004.07.004

Zouaghi, S., Six, T., Nuns, N., Simon, P., Bellayer, S., Moradi, S., Hatzikiriakos, S.G., André, C., Delaplace, G., Jimenez, M., 2018. Influence of stainless steel surface properties on whey protein fouling under industrial processing conditions. J. Food Eng. 228, 38–49. https://doi.org/10.1016/j.jfoodeng.2018.02.009